

September 20, 2004 ---- LA-UR-04-6702

Pre-Shot Report for September 2004 Omega Jet Shots

Participants: R. Coker, B.H. Wilde, P.A. Keiter (LANL); T. S. Perry, B. Blue (LLNL), J. M. Foster, P. A. Rosen (AWE).

Goals

The goals for the up-coming (29th September, 2004) shots are:

- 1) Quantify the hydrodynamic behavior of a directly-driven jet at various times.
- 2) Test the predictive capabilities of 2-D and 3-D simulations of hydrocodes from AWE (NYM/PETRA) and LANL (LASNEX/RAGE).
- 3) Determine the effects of target roughness and laser drive irregularity on the jets.
- 4) Field different diagnostic targets (nulls and foamless targets).
- 5) First demonstration of a late-time jet from an indirectly driven target (hohlraum).

Introduction

Many astrophysical objects, from young stars to active galactic nuclei, involve supersonic collimated jets. In view of the theoretical uncertainties in jet-forming mechanisms and limitations of numerical modeling of jet propagation, it is important to carry out jet experiments to further our understanding of the physics of jets in general.

In these experiments, we wish to radiograph a supersonic jet traveling through a low-density foam as a broad analogue of astrophysical jets. We use point projection X-ray radiography in order to achieve a large field of view late in time with sufficiently uniform illumination. In addition, we use titanium as the material driven by the laser to form the jet so as to provide good contrast with the vanadium backlighter; the He-like resonance line of vanadium lies just above the K-absorption edge of titanium.

An additional aim of this campaign is to study the transition to turbulence. The threshold for turbulence is a Reynolds number of about 2×10^4 . These experiments should have a Reynolds number significantly larger than this. Thus, if the jets are allowed to travel many times their original diameter, they should be seen to go turbulent. However, the high Mach number of these experiments at early times may mitigate the development of turbulence at late times. Past Omega experiments have shown extensive stirring in the jet; whether this is due to turbulence or poor initial conditions is not clear. Overall, these experiments will serve as a good verification problem for the hydrocodes.

Targets

The experiments will use 4 different primary target designs (3 jet direct-drive target types and 1 hohlraum target type) and 2 backlighter target designs.

The standard jet target consists of a 4 mm diameter titanium alloy washer with a central 300 μm diameter hole, followed by a 4 mm diameter, 6 or 2.5 mm long cylinder

of low density (nominally 0.1 g/cm^3) RF foam. The washer is $700 \mu\text{m}$ thick and has a $125\text{-}\mu\text{m}$ thick cap on top. On top of the Ti cap is a thin, gold washer ‘cookie cutter’ that is $50 \mu\text{m}$ thick with an inner diameter of $700 \mu\text{m}$. The exposed parts of the Ti cap and Au cookie cutter are coated with $4 \mu\text{m}$ of plastic (Parylene-N). A supersonic hydrodynamic jet is formed in the central hole and penetrates the foam cylinder at late time; the jet is diagnosed by point-projection X-ray backlighting. Coronal emission from the jet target assembly is shielded from the principal diagnostics by a $50\text{-}\mu\text{m}$ thick conical gold shield that is coated with $20 \mu\text{m}$ of Parylene-N. A 3D rendering of the target, including the illuminating laser bundles (see below) is shown in Fig. 1. A drawing showing the dimensions of the standard direct drive jet target and the placement of the fiducial gold grid is shown in Fig. 2a. Although it is possible that the jet may reach the grid at late times (see below), the grid is not placed further from the washer so that both the grid and washer edge are in the field of view of the primary diagnostic.

The second jet target type is a ‘null’. That is, these targets are identical to the standard jet target but with no free-run region. The Ti is a solid cylinder that is 3 mm in diameter and $825 \mu\text{m}$ thick. These ‘jet-less’ shots will serve as fiducials to characterize the effects of the roughness of the external Ti surfaces and the non-uniformity of the laser drive.

The third jet target type is ‘foamless’. They are identical to the standard jet targets but the foam will be removed on shot day. These shots will help determine if characteristics of the foam are primary drivers of the jet structure.

The fourth set of targets consists of gold hohlraums. They are standard jet targets with hohlraums attached on the drive side. The gold hohlraums are ‘standard’: $50 \mu\text{m}$ thick walls, $1600 \mu\text{m}$ wide, $1200 \mu\text{m}$ long with $1200 \mu\text{m}$ LEH and $800 \mu\text{m}$ drive hole. We expect the X-ray shielding to be effective but have not used the Au shield in conjunction with a hohlraum before. The cookie cutters for the hohlraum targets are $100 \mu\text{m}$ thick rather than $50 \mu\text{m}$ and have an inner diameter of $500 \mu\text{m}$ rather than $700 \mu\text{m}$. A drawing of the hohlraum jet targets is shown in Fig. 2b.

The four target sets will have a mixture of 6 mm (‘long’) and 2.5 mm (‘short’) foams. These foams are 3.25 mm in diameter (versus 4 mm for the March 2004 shots). The short foams will not have the fiducial gold grids attached. However, short foams will provide us with zero-points in the field of view to determine the illumination level of the backlighter. For these shots, the backside of the washer will serve as a spatial fiducial. Some of the ‘standard’ and ‘foamless’ targets will not have Au cookie cutters. Also, the Ti in the washers of all of the jet targets is actually a Ti/6Al/4V alloy, which is easier to machine; the $125\text{-}\mu\text{m}$ thick Ti cap is rolled and thus is pure Ti.

The backlighter target is a thin foil backed at a distance of $500 \mu\text{m}$ by a plastic coated ($20 \mu\text{m}$ of Parylene-N), $50\text{-}\mu\text{m}$ thick tantalum foil with a $20 \mu\text{m}$ pinhole to provide a source for point-projection imaging. In order to provide more uniform illumination, the pinholes have a taper such that they are $50 \mu\text{m}$ wide on one side; whether this is the drive side of the backlighter or not should not matter but we have not used tapered backlighters before during this campaign. The foil is a $50\text{-}\mu\text{m}$ thick and 5-mm square piece of plastic with an embedded $200\text{-}\mu\text{m}$ diameter “micro-dot” of vanadium (as shown in Fig. 3). The backlighter laser spot diameter will be nominally $600 \mu\text{m}$. The plasma created from the ablation of the plastic should constrain the expansion of the vanadium plasma and therefore help shield the diagnostic from the V plasma. The two backlighter target sets

will be the same except that the backlighters for the hohlraum targets will have a different angular orientation on the stalk (-11.8 instead of +19.5 degrees). A total of 20 backlighter targets will be made, 16 for the direct drive and 4 for the indirect drive shots. Another type of backlighter target using a 50- μm wide and 30- μm deep step-cut to get a 1:1 aspect ratio for the pinhole was to be made by LLNL but those backlighter targets will not be used for these shots.

The front, driven surface of the direct-drive jet target is in the $\phi=90$ deg plane and the target is offset by 10 mm from TCC towards H7. The backlighter pinhole is offset 10 mm towards H14 and 2.5 mm ‘downstream’ of the driven side of the target with the vanadium backlighter target 500 μm behind the pinhole. Given this target alignment, the resulting backlighter alignment details for the backlighter targets for the direct drive targets are given in Table 1a and for the indirect drive targets in Table 1b.

The Au cookie cutter in front of the Ti drive surface, combined with the XRFC used to view the drive side of the target, should aid us in aligning the target with the drive lasers. However, in the absence of a pointing ball shot, we will not know if any required offset is due to laser mispointing or target misalignment.

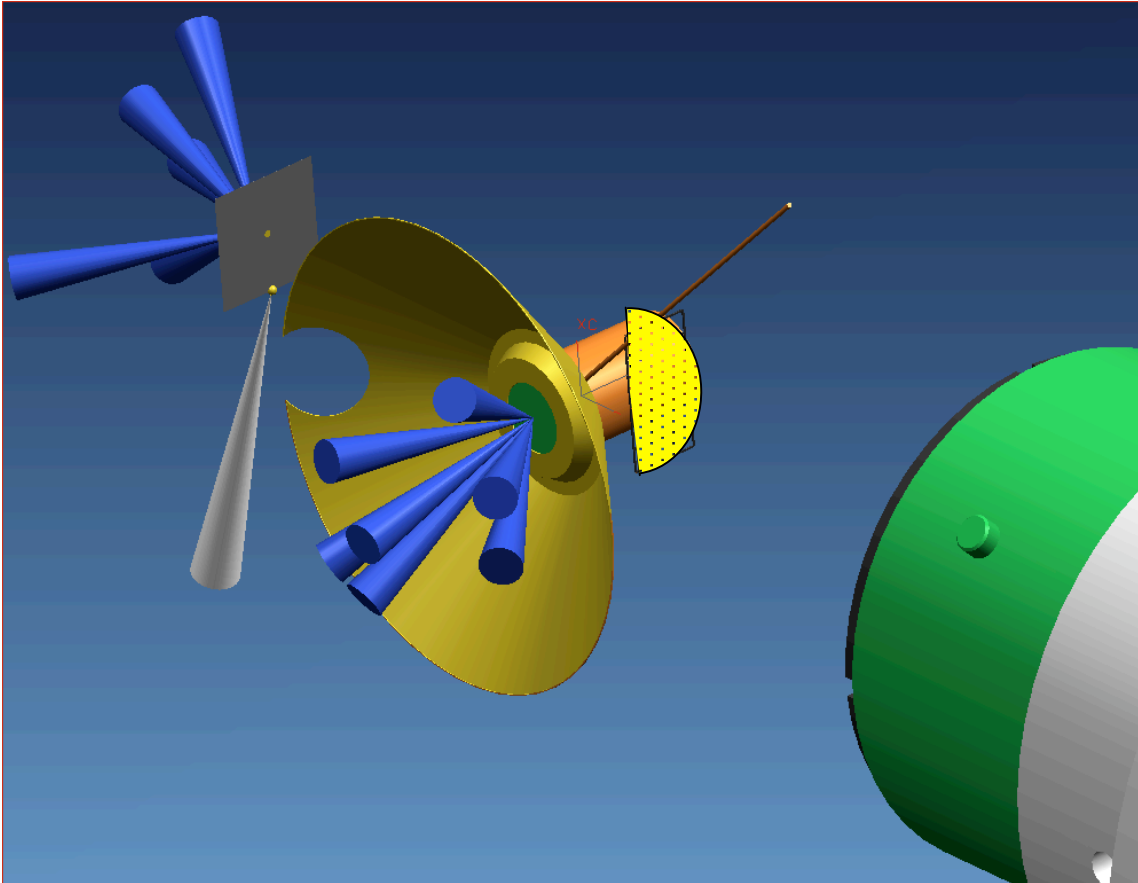


Figure 1: A three-dimensional drawing of the standard jet target in relation to the backlighter and the diagnostic (SPCA). The gold “cookie-cutter” is not included in the figure. The 2.5 mm long foams will not have a grid.

		Pointing	Pointing	Pointing
Backlighter size	Corner	R (mm)	θ (deg)	ϕ (deg)
5-mm square	1	11.674	97.0751	238.767
	2	10.776	97.668	258.909
	3	10.060	103.290	275.907
	4	10.998	118.929	252.185

Table 1a: Alignment parameters for the direct-drive backlighter targets.

		Pointing	Pointing	Pointing
Backlighter size	Corner	R (mm)	θ (deg)	ϕ (deg)
5-mm square	1	10.607	59.874	74.861
	2	10.607	77.529	97.312
	3	10.607	98.525	79.808
	4	10.607	82.084	57.980

Table 1b: Alignment parameters for the indirect-drive backlighter targets.

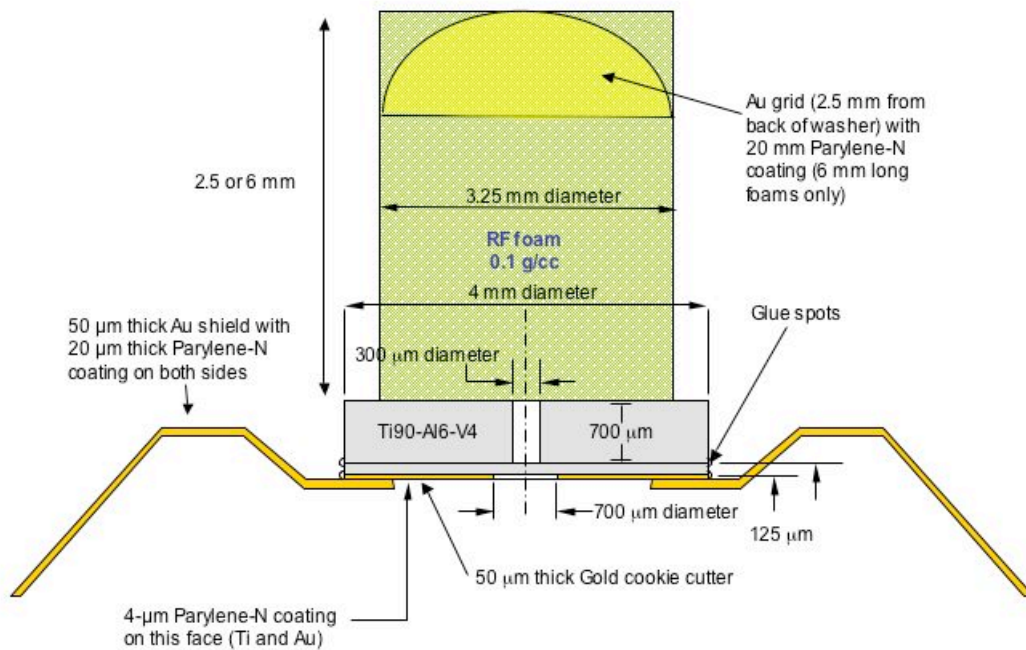


Figure 2a: A drawing of the standard jet target. The gold conical shield is not to scale.

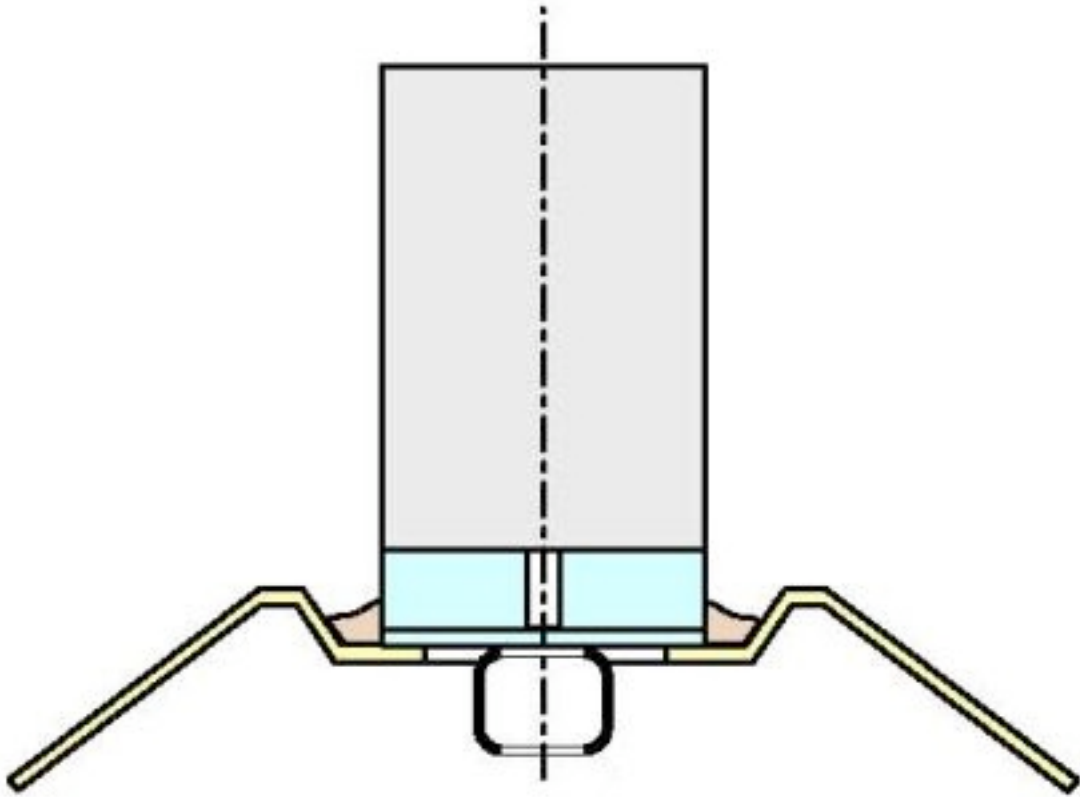


Figure 2b: A rough drawing of the hohlraum jet target. The cookie cutter and Ti are not CH coated. The Au grid and cookie cutter are not shown. In these shots, the diameter of the foam is 3.25 mm while the diameters of the washer and cap are 4 mm.

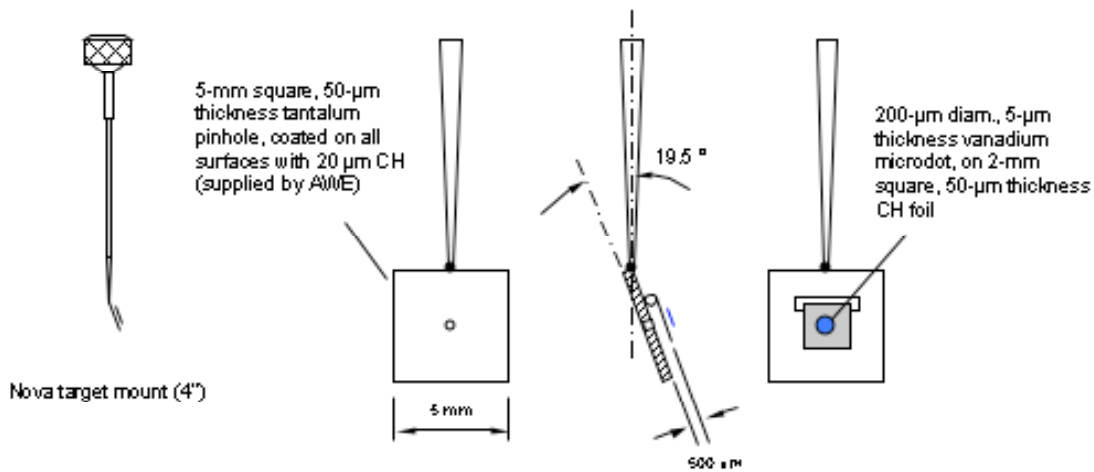


Figure 3: Drawings of the direct-drive backlighter target. Shown from left to right is the backlighter target mount, the front view of the backlighter target, the side view of the backlighter target and the rear view of the backlighter target. The backlighter foil is a 200 μm diameter, 5 μm thick piece of V mounted to a 2 mm square piece of CH and the pinhole substrate is a 5 mm square, 50 μm thick piece of Ta with a 20 μm diameter pinhole centered in it. The Ta substrate is also attached to the mount with a wire. The ‘CH’ is actually Parylene-N and is only 15 μm thick. The Parylene coating near where the target is attached to the stalk is removed to ensure good adhesion of the glue to the pinhole target. The hohlraum backlighters will have a bend of -11.8 degrees from the mounting stalk instead of $+19.5$ degrees.

Shot Sequence

The tentative shot sequence for the shots is shown in Table 2. This table assumes that data are being reliably obtained by the SPCA, the backlighter is nominal, and there are no surprises. We anticipate 9 shots (7 direct-drive and 2 indirect-drive) but if things go smoothly we may get a few more.

The first priority is to get a time history (spanning 0 to 400 ns) for the direct-drive standard jets. Before ~ 100 ns the jet is expected to be straight even with asymmetries and there are few good early-time diagnostics (e.g. the mach ring) to compare with the simulations. Next priority (particularly if the jets are still very 3D) is to have the nulls at an early (~ 100 ns) and late (~ 400 ns) time to see if we are at least getting the pedestal right (and the instability of the Ti interface can be used for mixing studies in its own right). Third priority (if the jet is not very 3D) is to get an early time of the jet, useful for determining jet velocity at early times (to be used predictively in future experiments and simulations). Fourth priority is a ‘repeatability’ shot at late time (but not so late that the grid needs to be removed) for the direct-drive standard jet; this is more important the more 3D the jets are. Next priority is the hohlraum test shots, one early in time and one late in time to see how a smooth drive changes the jet asymmetry. However, these shots are to be done last since switching from direct-drive to indirect-drive is expected to be slow and cost us at least one shot. Last priority is the foamless shots in order to determine the role of the foam in the jet asymmetry and to get a large area estimate of the

BL intensity. Note that any foamless shots will occur before the hohlraum shots in time.

Addendum: Due to time constraints, only 10 targets will be made. With an estimated 1.5 hrs for switching to indirect drive, we expect to get 9 shots, 7 direct and 2 indirect. With the targets listed in Table 2, we should have 4 short foams left over for the next series of shots. Shooting a null first will permit alignment of the drive beams and target (likely to be required unless the added alignment fiducial of the foams results in an offset) while getting useful information on the ‘pedestal’ without ‘wasting’ a jet target.

Shot #	Target	Foam	BL timing (ns)	Polished?
1	Null	Long	400	N
2	Jet Target	Long	200	Y
3	Jet Target	Long	300	Y
4	Jet Target	Short	100	Y
5	Jet Target	Long	400	Y
6	Jet Target	Long	300	Y
7	Null	Short	200	N
8	Hohlraum	Long	100	N
9	Hohlraum	Long	300	N
Spare	Hohlraum	Long	-	N

Table 2: A list of the preliminary shot and target sequence. Both the laser drive and backlighter drive will be on for all shots. The BL for shots at 400 ns are so late in time that the grid (if present) will need to be removed from the foam. All targets will have Au cookie cutters (though the hohlraum cookie cutters are different from the direct drive cookie cutters).

The Laser Beams

This experiment requires two-driver operation. Pulse shape for all beams will be 1 ns square. We will start with delaying the BL beams by 0 ns (to get a zero-time fiducial) and then increasing the delay to as much as 400 ns for subsequent shots. For these experiments, a difference of a few ns in the drive and BL times is not critical.

The drive beams for the direct-drive shots will be beams 20, 21, 27, 32, 35, 37, and 39. The pulse shape will be SG1014 for the drive beams; this should produce a ‘super-Gaussian’ that is nearly a square wave. These beams will have SG8 phase plates installed. These beams will be pointed at a point 10 mm away from TCC in the direction of TIM2 (that is, pointed at $r = 10.00$ mm, $\theta = 79.19$ degrees, $\phi = 90.00$ degrees). We would like to vary the drive beam energy in the range 200 – 450 J (each beam). The goal will be a total drive of 2240 J, corresponding to 320 J per beam for all 7 beams and a peak intensity of 4×10^{14} W/cm². It may be necessary to defocus the beams to get a smoother spatial profile.

The drive beams for the hohlraum shots will be 51, 69, 25, 50, 54, 58, 59, 60, 63, 64, 65, and 67. The pulse shape will be SG1014 for these drive beams as well. They will heat a hohlraum on the P7-P6 axis (laser entry hole in the P7 end). Beams 51 and 69 lie on a 42.02 degree cone relative to the hohlraum axis; all other drive beams lie on a 58.85 degree cone. The laser spots must be small enough to ensure the edge of the LEH is not clipped; thus, we request **NO** phase plates be in place for the drive beams. Drive-beam energy will be fixed at 450 J per beam, and not varied between shots; energy balance

should be as good as can reasonably be obtained. The drive beams will be pointed approximately 10 mm from TCC, in the direction towards TIM5; precise beam pointing coordinates have been chosen to provide a balance between uniformly-distributed laser spots at the hohlraum wall and clipping the LEH.

The backlighter beams for the direct-drive shots will be beams 16, 41, 43, 48, and 49. Pulse shape SG1018 will be used for these beams. Beams 43 and 49 will have SG4 phase plates; beams 16, 41, and 48 will not have phase plates. These beams will be pointed at $r = 10.79$ mm, $\theta = 100.51$ degrees, and $\phi = 256.37$ degrees. Beams 16, 41 and 48 (no phase plates) will be defocused. Note the importance of the approx. 20.5-mm separation between main target and backlighter target; this is necessary to give the required field of view for the experiment. Time delay between the main and backlighter beams will be in the range 0-400 ns. The chosen focus of -3.72 mm for the beams without phase plates should result in a backlighter beam spot size of 600 μm . Nominally, we will only be using the two beams with phase plates (43 and 49, the beams with the most normal incidence to the BL) with 450 J/beam; the other 3 beams are in case we require a higher BL intensity.

The backlighter beams for the indirect-drive shots will be beams 11, 13, 14, 18, and 47. SG4 phase plates are to be used for beams 13 and 18; beams 11, 14, and 47 will not have phase plates. As in the direct drive case, we plan on initially using only the two most perpendicular backlighter beams (those two with phase plates) with beam energies of 450 J (each beam). The backlighter beams will be pointed at approximately 10 mm from TCC, in the direction towards TIM2. Time delay between the indirect drive and backlighter beams will be in the range 0–400 ns (backlighter delayed).

Power/energy balance is not critical for either the drive or the backlighter beams. A summary of the drive and backlighter beam details for the direct-drive shots is given in Table 3a and for the indirect-drive shots in Table 3b. Note that the indirect-drive shots will have the target turned around roughly 180 degrees compared to the direct-drive shots.

Beam	Energy (J)	Pointing			Focusing (mm)	DPP	Termination
		R (mm)	Theta (deg)	Phi			
16	0	10.79	100.51	256.37	-3.72	NO	Backlighter
41	0	10.79	100.51	256.37	-3.72	NO	Backlighter
43	450	10.79	100.51	256.37	0	SG4	Backlighter
48	0	10.79	100.51	256.37	-3.72	NO	Backlighter
49	450	10.79	100.51	256.37	0	SG4	Backlighter
20	320	10	79.19	90	0	SG8	Target
21	320	10	79.19	90	0	SG8	Target
27	320	10	79.19	90	0	SG8	Target
32	320	10	79.19	90	0	SG8	Target
35	320	10	79.19	90	0	SG8	Target
37	320	10	79.19	90	0	SG8	Target
39	320	10	79.19	90	0	SG8	Target

Table 3a: A list of the backlighter and drive beam parameters used in the direct-drive jet experiments. The energies listed are nominal values; they may end up being varied from 200-450 J/beam. All beams will have DPR on.

Beam	Energy (J)	Pointing			Focusing (mm)	DPP	Termination
		R (mm)	Theta (deg)	Phi			
11	0	10.50	79.19	77.50	-3.72	NO	Backlighter
13	450	10.50	79.19	77.50	0	SG4	Backlighter
14	0	10.50	79.19	77.50	-3.72	NO	Backlighter
18	450	10.50	79.19	77.50	0	SG4	Backlighter
47	0	10.50	79.19	77.50	-3.72	NO	Backlighter
51	450	10.77	109.89	236.91	-0.3	NO	Target
69	450	10.77	109.89	236.91	-0.3	NO	Target
25	450	10.66	109.34	238.39	-0.75	NO	Target
50	450	10.66	109.34	238.39	-0.75	NO	Target
54	450	10.66	109.34	238.39	-0.75	NO	Target
58	450	10.66	109.34	238.39	-0.75	NO	Target
59	450	10.66	109.34	238.39	-0.75	NO	Target
60	450	10.66	109.34	238.39	-0.75	NO	Target
63	450	10.66	109.34	238.39	-0.75	NO	Target
64	450	10.66	109.34	238.39	-0.75	NO	Target
65	450	10.66	109.34	238.39	-0.75	NO	Target
67	450	10.66	109.34	238.39	-0.75	NO	Target

Table 3b: A list of the backlighter and drive beam parameters used in the indirect-drive jet experiments. The energies listed are nominal values; they may end up being varied from 200-450 J/beam. All beams will have DPR on.

Diagnostics

A general diagnostics summary is shown in Table 4a for the direct-drive shots and in Table 4b for the indirect-drive shots.

Direct Drive: The diagnostic in TIM 1 will be X-ray Pinhole Camera 3, with a magnification of 4 and a pinhole diameter of 11 μm . It will contain film or CID and will take a time-integrated image of the main-target side of the backlighter pinhole. This diagnostic can be omitted if there are only two XRPHCs available. TIM 5 will hold XRPHC 1, also with a magnification of 4 and a pinhole diameter of 11 μm . It will contain film or CID and take a time-integrated image of the backlighter-target assembly, viewed from the vanadium microdot side. TIM 6 will contain XRPHC 2 with a magnification of 4 and a pinhole diameter of 11 μm . It will contain film or CID and take a time-integrated image of the backlighter-target assembly, viewed edge on. The diagnostic in TIM 4 will be X-ray Framing Camera 1, with a magnification of 6, a pinhole diameter of 10 μm , a 100 ps pulse former, a bias of 200 V, and timing intervals of 0.5 ns. It will contain film and be aligned to the drive beams so as to observe beam uniformity and alignment relative to the hole in the Au cookie cutter or cross-wires.

The SPCA (Static Pinhole Camera Array) in TIM 2 is the principal diagnostic and will record a point-projection radiograph of the jet in the target foam 2.5 mm downstream from TCC. It will use an AWE special snout and nose cone and will use DEF film. The SPCA will use a 9 mm diameter Ta aperture as for the previous shots in March 2004.

Fig. 4 shows the XTVS and YTVS views. These will be useful in aligning the diagnostics. Figs. 5-9 show the pointing of each of the diagnostics. The views were generated from the VisRad software from a vantage point of 9 cm away.

Indirect Drive: The indirect drive diagnostics will be very similar to the direct drive diagnostics. In the future, we would like to use DANTE, configured to view the P7-end of the hohlraum LEH, at 190 eV for indirect drive shots. However, the present target setup would require a 4 mm shift to have the entire hohlraum in the 10 mm FOV of DANTE.

The diagnostic in TIM 1 will be X-ray Pinhole Camera 3, with a magnification of 4 and a pinhole diameter of 11 μm . It will contain film or CID and will take a time-integrated image of the backlighter-target assembly, viewed from the vanadium microdot side. This diagnostic can be omitted if there are only two XRPHCs available. TIM 2 will hold XRPHC 1, also with a magnification of 4 and a pinhole diameter of 11 μm . It will contain film or CID and take a time-integrated image of the main-target side of the backlighter pinhole. TIM 4 will contain XRPHC 2 with a magnification of 4 and a pinhole diameter of 11 μm . It will contain film or CID and take a time-integrated image of the backlighter-target assembly, viewed edge on. The diagnostic in TIM 6 will be XRFC 1, with a magnification of 6, a pinhole diameter of 10 μm , a 100 ps pulse former, a bias of 200 V, and timing intervals of 0.5 ns. It will contain film and be aligned to the laser-entry hole of the hohlraum so as to check for beam clipping. To assist with alignment, Fig. 10 show the location of the hohlraum target in the target chamber, Fig.

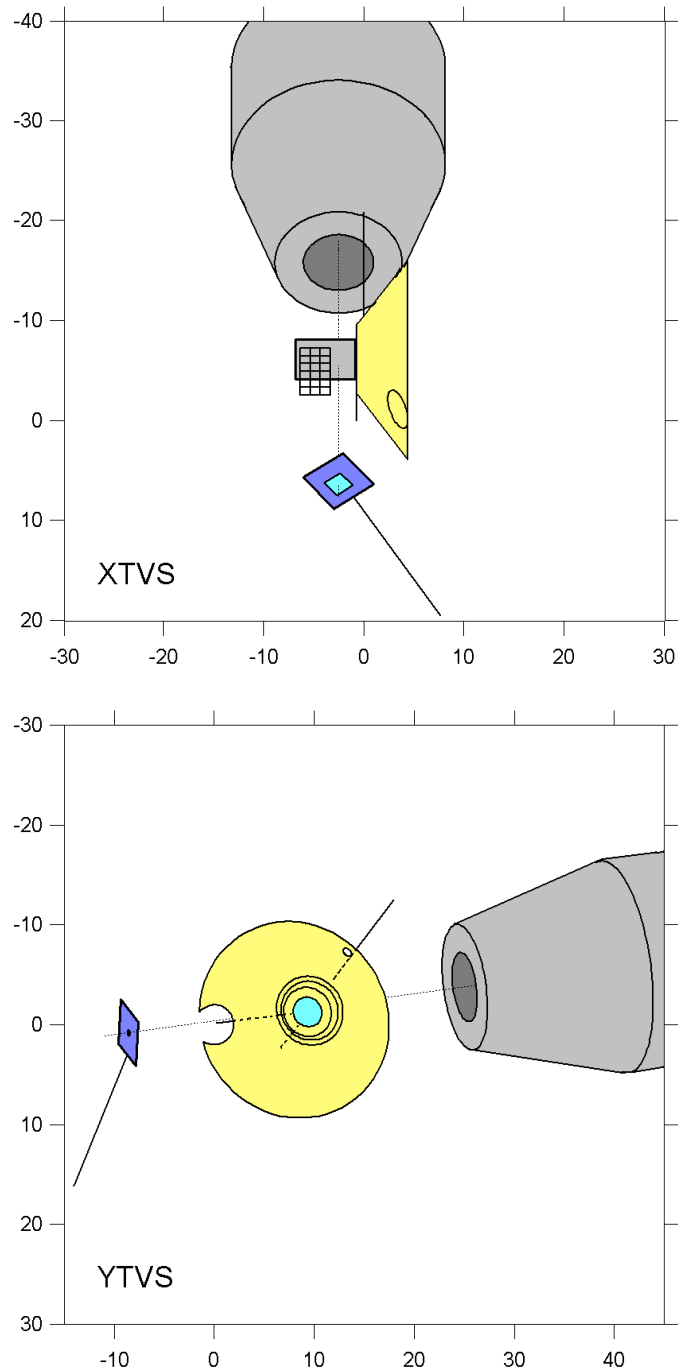
11a shows the XTVS and YTVS views for the hohlraum target, and Fig. 11b shows the hohlraum target as seen by the diagnostics in the TIMs.

The SPCA in TIM 5, aligned to TCC, is the principal diagnostic and will record a point-projection radiograph of the jet. It will use an AWE special snout and nose cone and will use DEF film. The SPCA will use a 9 mm diameter Ta aperture as for the previous shots in March 2004 but will be on a swing mount for proper alignment.

TIM	Diagnostic	Pointing			Filters	Priority
		R (mm)	θ (deg)	ϕ (deg)		
1	XRPHC 3	10.79	100.51	256.37	0.02" Be – Front 0.001" Be - Rear	Tertiary
2	SPCA	2.5	90.0	180.0	0.02" Be & 0.001" V – Front 0.01" Be – Rear	Primary
3	LLNL Target Positioning System	-	-	-	-	Primary
4	XRFC 2	10.0	79.19	90.0	0.02" Be – Front 0.001" Be - Rear	Primary
5	XRPHC 1	10.79	100.51	256.37	0.02" Be – Front 0.001" Be - Rear	Secondary
6	XRPHC 2	10.79	100.51	256.37	0.02" Be – Front 0.001" Be - Rear	Secondary

Table 4a: A list of the diagnostics used in each TIM for the direct drive jet experiments.

TIM	Diagnostic	Pointing			Filters	Priority
		R (mm)	θ (deg)	ϕ (deg)		
1	XRPHC 3	10.50	79.19	77.50	0.02" Be – Front 0.001" Be - Rear	Tertiary
2	XRPHC 1	10.50	79.19	77.50	0.02" Be – Front 0.001" Be - Rear	Secondary
3	LLNL Target Positioning System	-	-	-	-	Primary
4	XRPHC 2	10.50	79.19	77.50	0.02" Be – Front 0.001" Be - Rear	Secondary
5	SPCA w/ swing mounting	TCC	-	-	0.02" Be & 0.001" V – Front 0.01" Be – Rear	Primary



6	XRFC 1	10.70	109.53	237.89	0.02" Be – Front 0.001" Be - Rear	Primary
---	--------	-------	--------	--------	--------------------------------------	---------

Table 4b: A list of the diagnostics used in each TIM for the indirect drive jet experiments.

Figure 4: The views from the XTVS (top) and YTVS (bottom) for the direct drive targets. The axes are labeled in units of mm.

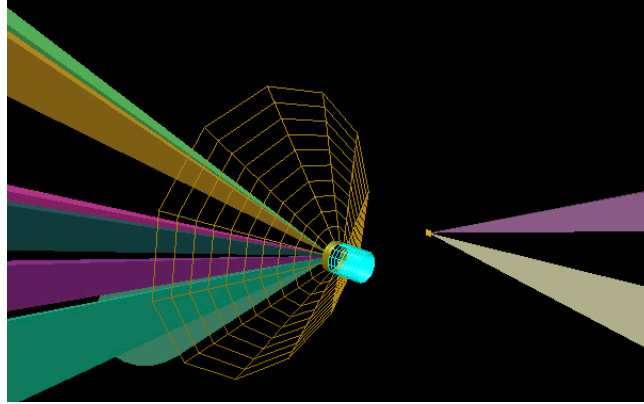


Figure 5: The view for the direct-drive shots of the XRPHC 3 in TIM 1 from 9 cm. It is observing the backlighter. The image will be a time-integrated image of the backlighter pinhole. We wish to determine if the pinhole substrate lights up, especially on its sharp corners.

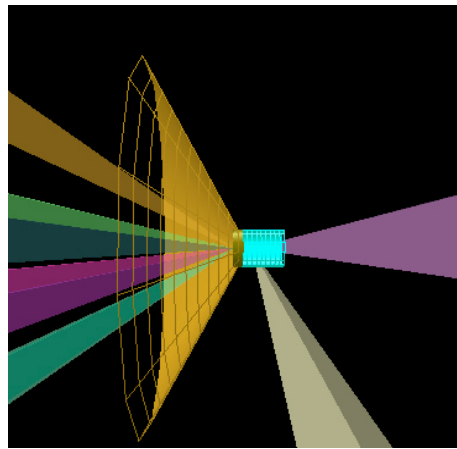


Figure 6: The view for the direct-drive shots of the SPCA in TIM 2 from 9 cm. This is the primary instrument and records the radiograph of the jet.

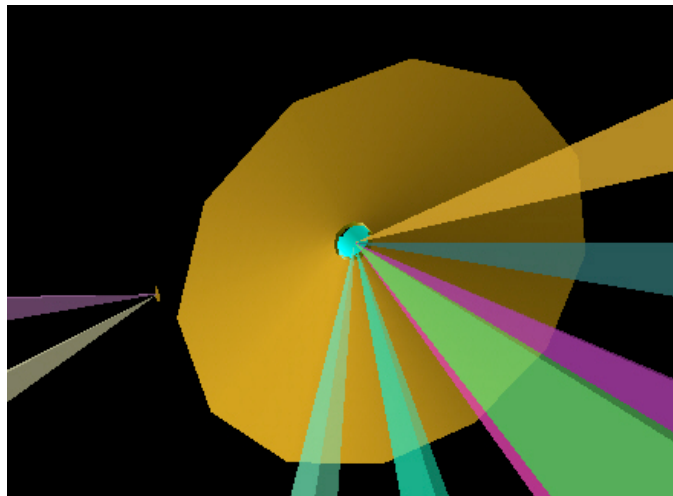


Figure 7: The view for the direct-drive shots of the XRFC 2 in TIM 4 from 9 cm. It is observing the drive-side surface of the jet target. This will be used to determine the temporal and spatial profile of the drive beams.

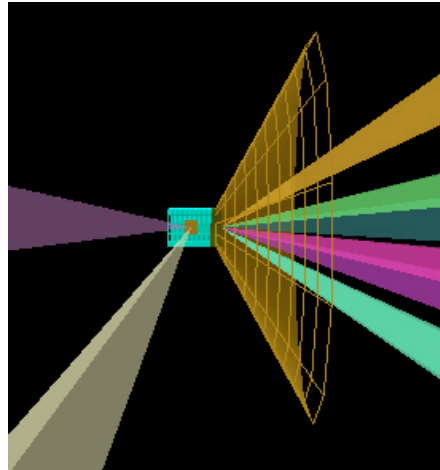


Figure 8: The view for the direct-drive shots of the XRPHC 1 in TIM 5 from 9 cm. It is observing the vanadium backlighter and will help provide information on the spot size.

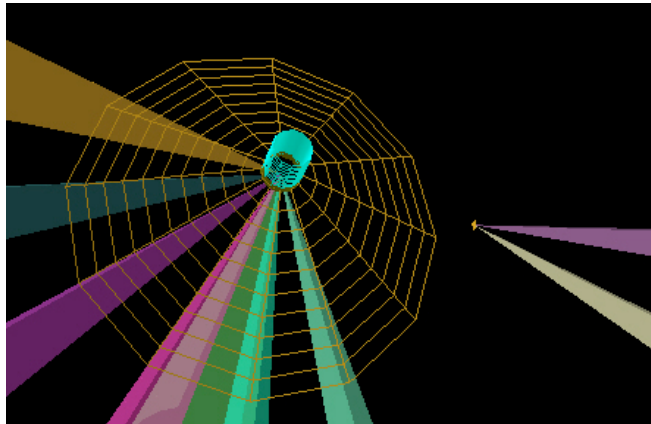


Figure 9: The view for the direct-drive shots of the XRPHC 2 in TIM 6 from 9 cm. It will be observing the backlighter side-on to measure the plasma expansion coming off of the backlighter.

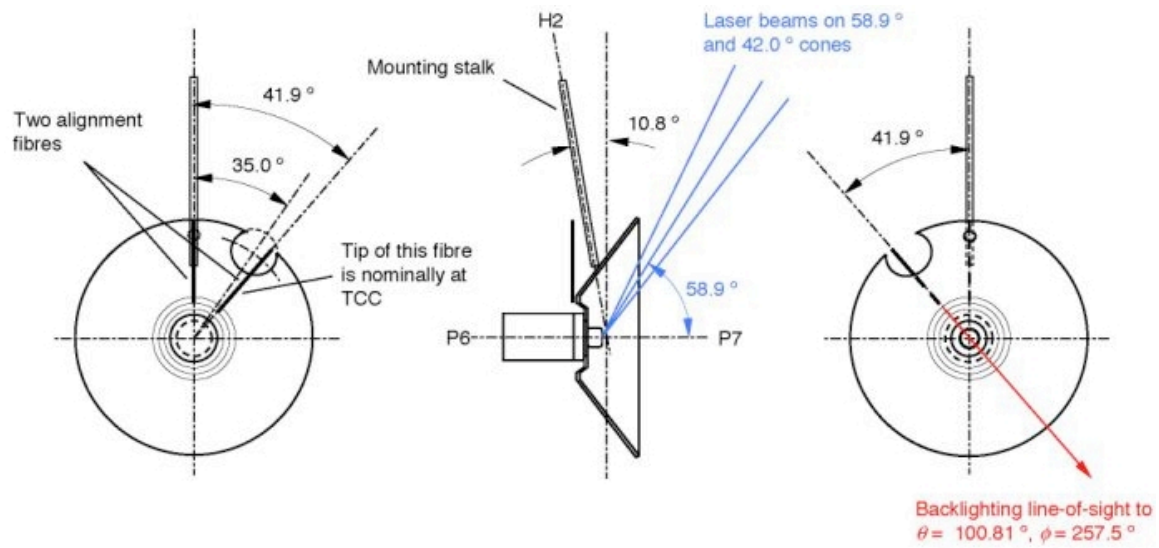


Figure 10: Figures showing the location of the hohlraum target in the chamber.

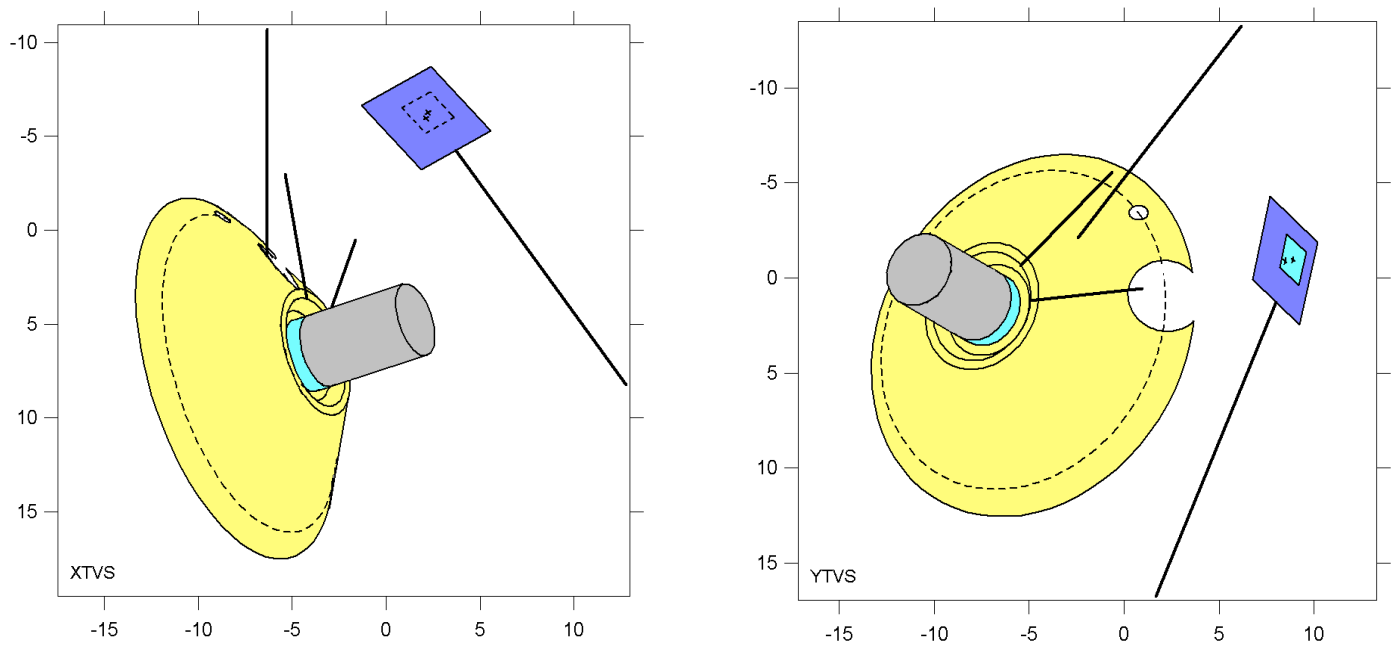


Figure 11a: Figures showing the XTVS and YTVS views for the hohlraum targets.

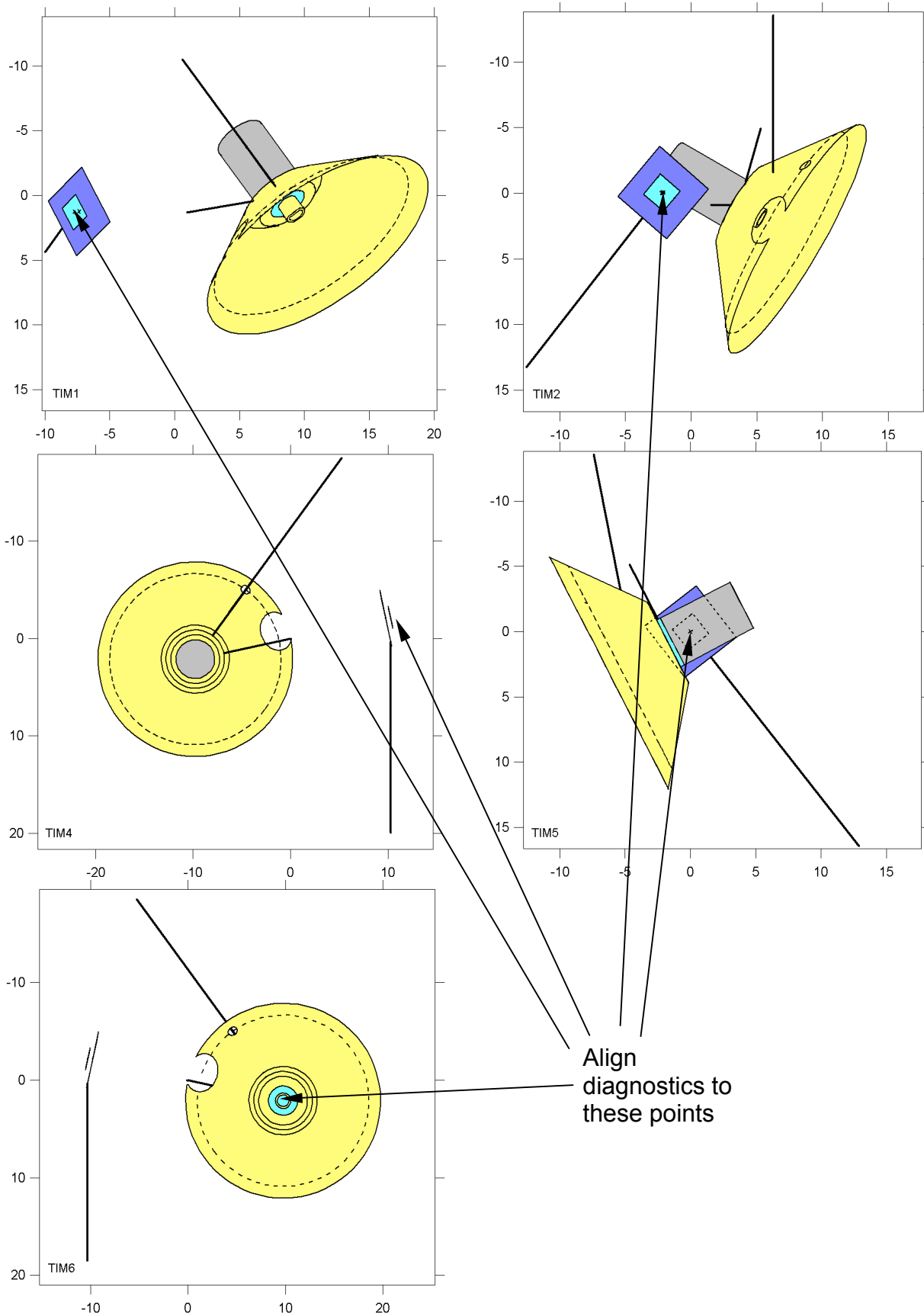


Figure 11b: Figures showing the hohlraum target as viewed from the various diagnostics.

Design Simulations

Design simulations have been carried out using Lagrangian codes (NYM and LASNEX) linked to Eulerian codes (PETRA and RAGE). Typical results are shown in Fig. 12. A series of collimated and pulsing jets are expected. The simulations lack the resolution at this point to be sure, but turbulence in the roll-up mushrooms may be seen at late times. Results of a linked LASNEX/RAGE calculation that more closely matches the conditions of these shots are shown in Fig. 13. Note the similarity to the left image in Fig. 12. These simulations indicate that the very tip of the jet, which propagates nearly linearly with time, will reach the front of the fiducial grid at 200 ns. With 7 drive beams, the low energy setting (200 J/beam) results in 1.4 kJ and the high energy setting (450 J/beam) in 3.15 kJ. Since the jet location also scales nearly linearly with laser intensity, the low drive will result in a jet reaching the grid at ~ 400 ns. Our nominal drive of 2.2 kJ should produce a jet that reaches the grid at ~ 300 ns. Fig. 14 shows a radiograph of a RAGE simulation for the hohlraum targets. The jet is somewhat larger than the direct drive jets at the same point in time. According to the simulations, indirect drive also produces a more mixed type of jet, particularly at early times, than direct drive. In any case, in the absence of 3D smearing due to turbulence or asymmetry in the drive, the simulated radiographs indicate we should be able to clearly see the interior structure of both the directly and indirectly driven jets with the V point-projection backlighter.

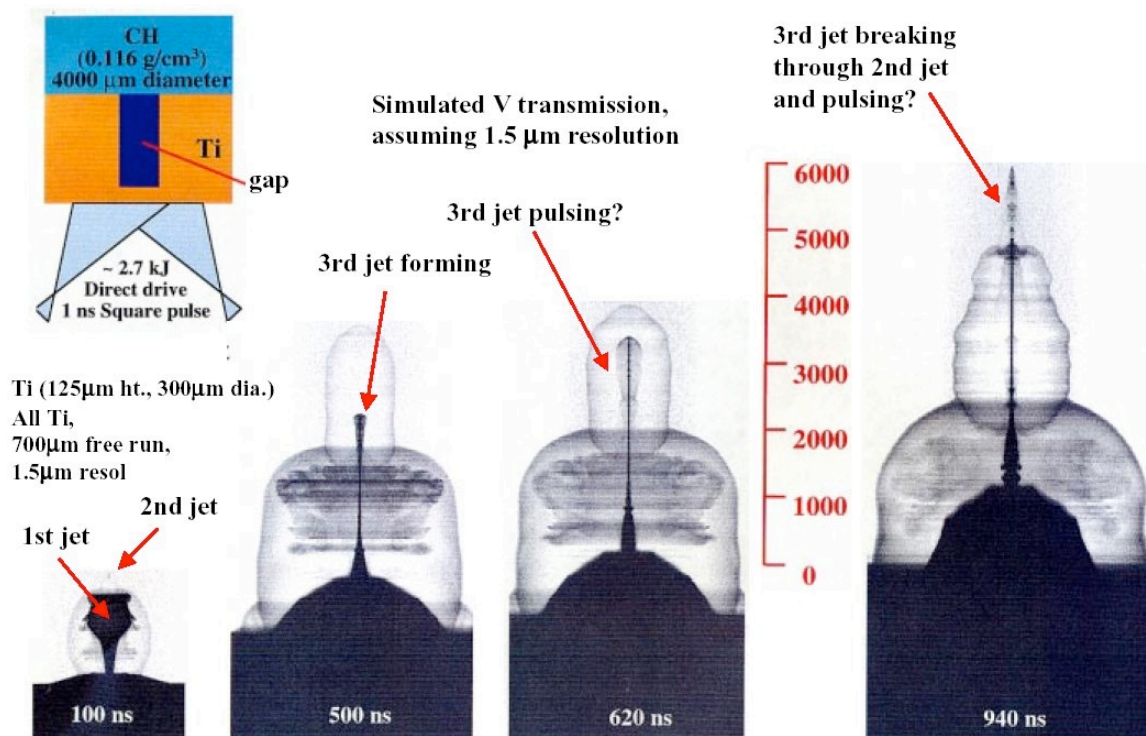


Figure 12: Typical simulation results for the September 2004 experimental setup. The images are simulated X-ray transmission radiographs. The scale bar is in μm . This particular simulation is an unlinked RAGE calculation that uses a temperature source and does not include the $4 \mu\text{m}$ coating on the Ti

cap. The density of the foam and equivalent total energy in the laser for this simulation (~2.7 kJ) may not match what we will be using for these shots (~2.2 kJ).

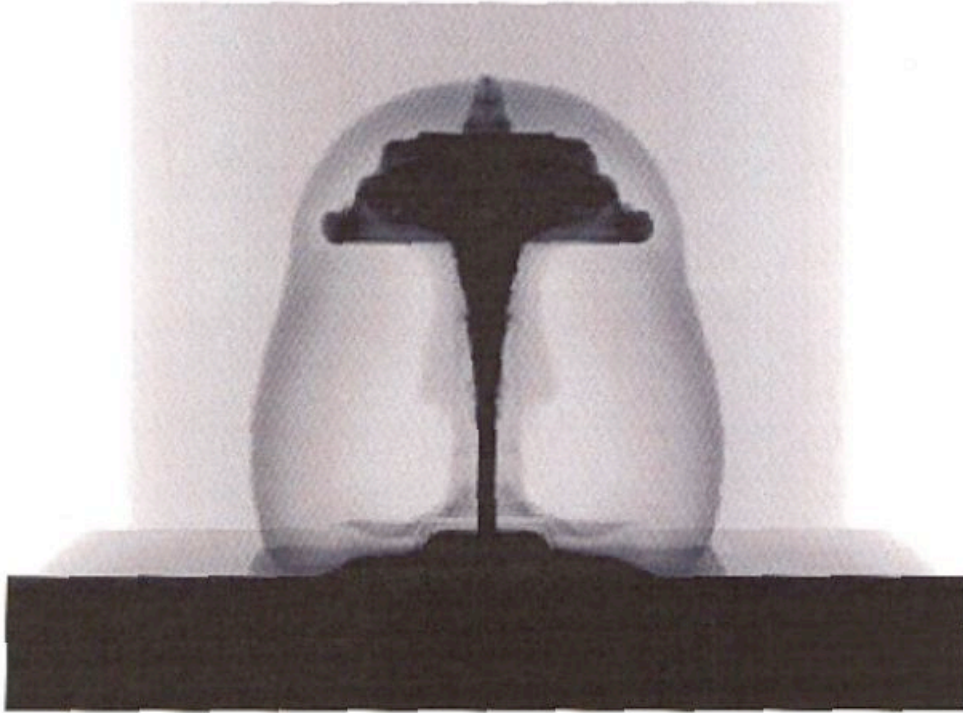


Figure 13: A simulated radiograph from a linked LASNEX/RAGE calculation (b17a4) with $3\ \mu\text{m}$ resolution using a 2.8 kJ laser energy and including the $4\ \mu\text{m}$ coating on the Ti. In this $4\times 3\ \text{mm}$ image, the calculation has reached 200 ns and the peak of the jet is 2.5 mm from the edge of the washer; thus it has just reached the grid. The link was done at 2 ns, after the laser is off. The image is scaled so that regions with transmission greater than 0.5 are white.

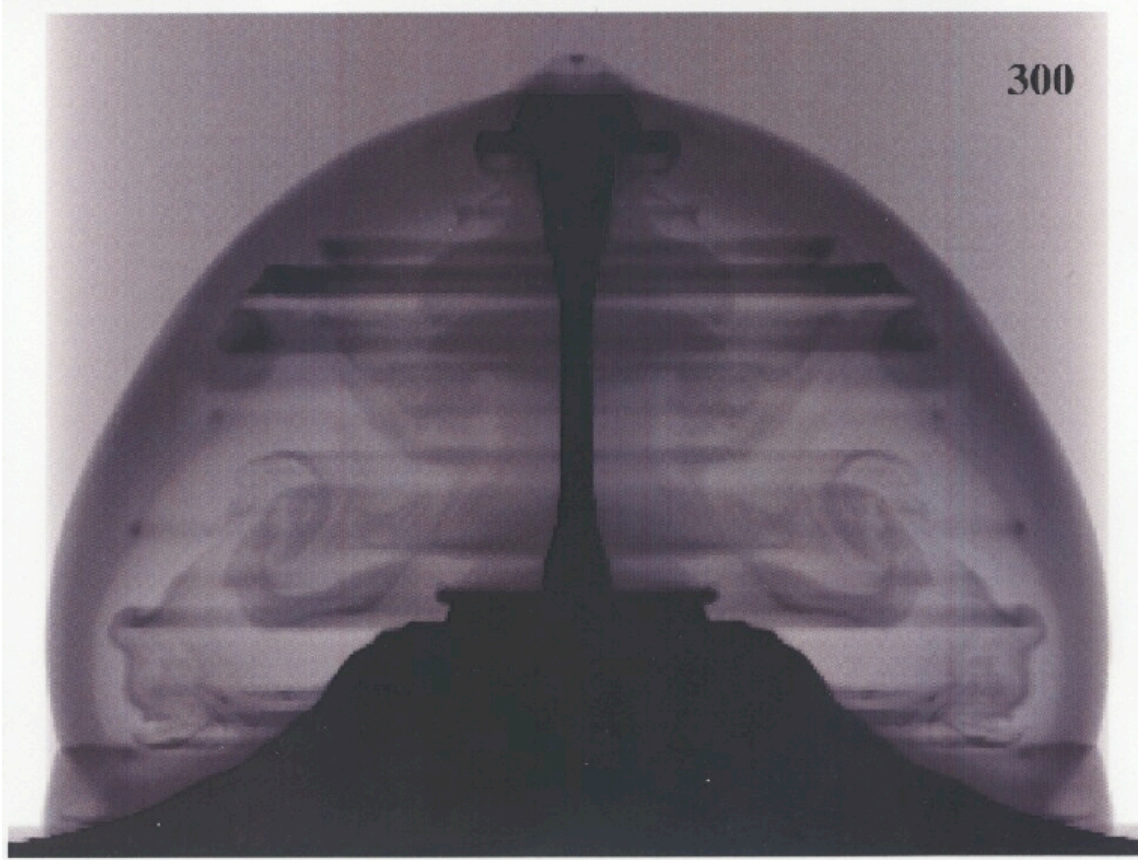


Figure 14: A simulated radiograph from a RAGE calculation with 3 μm resolution using a temperature source equivalent to 5.4 kJ of laser energy driving a hohlraum. It does not include the 4 μm coating on the Ti cap. In this 4x3 mm image, the calculation has reached 300 ns and the peak of the jet is 3 mm from the edge of the washer; thus it has passed the Au grid. The jet is 'brainier' and larger than the direct drive jet at the same time.